

# Mutual Learning for Acoustic Matching and Dereverberation via Visual Scene-driven Diffusion

Jian Ma<sup>1,3</sup>, Wenguan Wang<sup>2†</sup>, Yi Yang<sup>2</sup>, and Feng Zheng<sup>1</sup>

<sup>1</sup>Southern University of Science and Technology

<sup>2</sup>ReLER, CCAI, Zhejiang University <sup>3</sup>ReLER, University of Technology Sydney

<https://hechang25.github.io/MVSD>

**Abstract.** *Visual acoustic matching (VAM)* is pivotal for enhancing the immersive experience, and the task of *dereverberation* is effective in improving audio intelligibility. Existing methods treat each task independently, overlooking the inherent reciprocity between them. Moreover, these methods depend on paired training data, which is challenging to acquire, impeding the utilization of extensive unpaired data. In this paper, we introduce MVSD, a mutual learning framework based on diffusion models. MVSD considers the two tasks symmetrically, exploiting the reciprocal relationship to facilitate learning from inverse tasks and overcome data scarcity. Furthermore, we employ the diffusion model as foundational conditional converters to circumvent the training instability and over-smoothing drawbacks of conventional GAN architectures. Specifically, MVSD employs two converters: one for VAM called reverberator and one for dereverberation called dereverberator. The dereverberator judges whether the reverberation audio generated by reverberator sounds like being in the conditional visual scenario, and vice versa. By forming a closed loop, these two converters can generate informative feedback signals to optimize the inverse tasks, even with easily acquired one-way unpaired data. Extensive experiments on two standard benchmarks, *i.e.*, SoundSpaces-Speech and Acoustic AVSpeech, exhibit that our framework can improve the performance of the reverberator and dereverberator and better match specified visual scenarios.

**Keywords:** Visual acoustic matching · Dereverberation · Audio style transfer · Mutual learning · Diffusion

## 1 Introduction

Sound interacts with its environment, giving listeners a sense of objects and spatial imprints [75]. Reverberation is sound lingering in a space from surfaces reflecting sound waves [17, 37]. Thus, reverberant sound, faithfully replicating real-world acoustics, is vital for realistic and immersive experiences in applications like augmented and virtual reality [7, 31, 40, 45, 47, 79, 83]. Although reverberation can bestow a realistic sense of space, it may make speech content less intelligible [36, 61]. In line with human perception, automatic speech

---

<sup>†</sup> Corresponding author: Wenguan Wang.

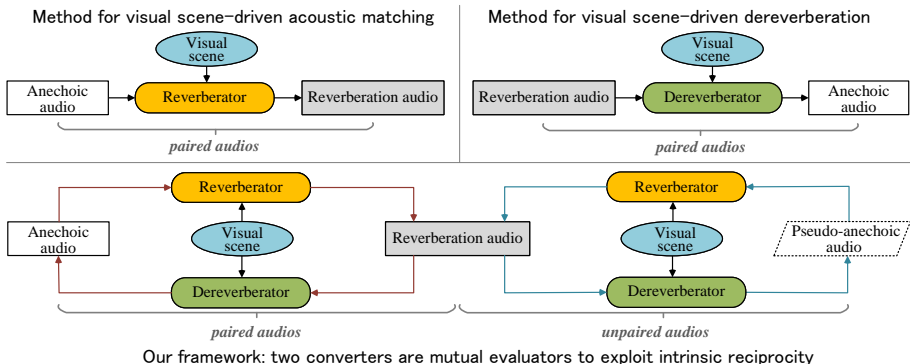


**Fig. 1:** There exists an inherent reciprocity between VAM and dereverberation. Unlike previous approaches that treat these two tasks independently, our framework simultaneously handles the both tasks. Forming a closed loop between the two converters can generate informative feedback signals to optimize the inverse tasks, even with easily acquired one-sided unpaired data (§1).

recognition systems also suffer from lower accuracy when processing reverberant speeches [12, 21, 80]. Therefore, dereverberation techniques [53] can benefit applications such as teleconferencing, hearing aids, voice assistants, *etc.* Existing works train VAM and dereverberation separately [4, 6, 15, 19, 68, 71]. The traditional methods of acoustic matching primarily involve unraveling the spatial characteristics of sound through the examination of Room Impulse Responses (RIRs), which assess the propagation and variation of sound within a specific environment [2, 3, 16, 52, 64, 71]. Rather than estimating RIRs, VAM [4] directly achieves specified reverberation by employing images of the target environment and original audio clips. For dereverberation, classical methodologies often encompass the application of signal processing and statistical techniques [54, 55], recent advances highlight neural network-based approaches that learn transfer functions from reverberation to anechoic spectrograms [12, 14, 22, 81]. Nonetheless, optimizing each task individually fails to leverage the inherent reciprocity between the two tasks (Fig. 1). Moreover, training these methods usually requires extensive paired data. Yet capturing large volumes of aligned anechoic and reverberant audio pairs in real-world scenarios is not feasible. For VAM, the shortage of paired audio usually leads to average-style reverberation. When it comes to dereverberation, the model struggles to produce highly ‘clean’ audio in response to complex scenarios. Thus, existing methods often face challenges in leveraging extensive unpaired audio due to the varying reverberation levels.

In this paper, we consider dereverberation as the inverse task of VAM, serving as an evaluator to provide feedback signals for VAM training, and vice versa. Specifically, given a visual environment  $\mathbf{v}$ , an anechoic audio  $\mathbf{a}_c$ , and a reverberant audio  $\mathbf{a}_r$ , VAM reverberator  $f_\theta(\mathbf{v}, \mathbf{a}_c) \rightarrow \hat{\mathbf{a}}_r$  maps the visual observation and anechoic audio into reverberant audio, while the dereverberator  $g_\phi(\mathbf{v}, \mathbf{a}_r) \rightarrow \hat{\mathbf{a}}_c$  restores reverberant audio to anechoic audio conditioned on visual characteris-

tics. There exists a solid reciprocal relationship between the input and output spaces of  $f_\theta$  and  $g_\phi$ . In this study, we delve into exploiting their intrinsic reciprocity to overwhelm the scarcity of parallel data. We propose a Mutual learning mechanism based on Visual Scene-driven Diffusion (MVSD) (Fig. 1). In MVSD, two converters, namely reverberator and dereverberator, are employed and capable of learning from the symmetric tasks. Taking VAM as an example, the reverberator, conditioned on the visual scene  $\mathbf{v}$ , simulates environmental acoustic effects and converts anechoic audio  $\mathbf{a}_c$  to reverberant audio  $\hat{\mathbf{a}}_r$ . Since the output of one converter can be used as the input for another, the reverberator and dereverberator can act as mutual evaluators. Concretely, in the primal task VAM, the reverberator generates reverberated audio  $\hat{\mathbf{a}}_r$  conditioned on the visual scene  $\mathbf{v}$  and anechoic audio  $\mathbf{a}_c$ . Then the reverse converter  $g_\phi$  takes  $\hat{\mathbf{a}}_r$  as input and reconstructs the anechoic audio  $\tilde{\mathbf{a}}_c$  within the symmetric dereverberation task. Finally, the errors between  $\tilde{\mathbf{a}}_c$  and  $\mathbf{a}_c$  are used as feedback signals to optimize reverberator  $f_\theta$ , and vice versa. The training process of reverberator  $f_\theta$  and dereverberator  $g_\phi$  can form a closed loop, providing feedback for inverse tasks to enhance data efficiency. When the dereverberator encounters a unpaired natural audio  $\mathbf{a}'_r$  with reverberation, it first eliminates the reverberation factors and creates a pseudo-anechoic audio  $\hat{\mathbf{a}}'_c$ . Likewise, the reverberator regenerates  $\tilde{\mathbf{a}}'_r$  based on  $\hat{\mathbf{a}}'_c$  and visual observations  $\mathbf{v}'$ . Hence, MVSD allows these two converters to benefit from each other’s training instances and can be extended to easily acquired unpaired audio samples. For conditional generation, the architecture built on GANs is presently the prevailing choice [8, 20, 27, 28, 49, 60]. However, the training of GAN may introduce potential risks of instability and over-smoothing. Diffusion model [1, 9, 10, 25, 41, 43, 48, 63] recently show remarkable milestones in image generation, enabling the creation of high-quality images based on conditioning cues. Some works introduce diffusion into audio generation, such as converting spectrograms into sound signals [35], generating symbolic music [50], *etc.* However, diffusion generation of specified reverberation styles under visual guidance remains underexplored. To bridge this gap, we meticulously devise a visual scene-driven diffusion model to mitigate the computational overhead. Specifically, the diffusion model for each task includes a visual scene encoder for extracting features to control reverberation style, and a controllable Unet that serves as the generator for producing the desired audio. Additionally, cross-modal attention is adopted in selective blocks to establish correlations between visual cues and audio, reducing computational demands.

We spotlight the notable strengths of MVSD in visual-audio cross-modal style transfer. MVSD effectively enhances the performances and consistently reports promising results on both tasks. We achieve a remarkable reduction of 0.157 in STFT-distance on the ‘Seen’ test set of SoundSpaces-Speech [4] (23.6% relative performance). Moreover, the utilization of unpaired audios (17.3% of the training data) can further boost the relative performance by 9.1% in RTE for VAM.

To summarize, the main contributions of this paper are as follows:

- We initially propose an end-to-end approach that leverages the reciprocity between VAM and dereverberation tasks to reduce reliance on paired data.

- We introduce a new and elegant mutual learning framework, MVSD, incorporating diffusion models and utilizing symmetrical tasks as evaluators to provide feedback signals to facilitate model training.
- We conduct a comprehensive evaluation of MVSD, demonstrating its superiority and confirming the potential of unpaired data in real-world applications.

## 2 Related Work

**Acoustic Matching.** Acoustic matching involves modifying audio to simulate the sound in a given environment. Schroeder *et al.* [65] first propose the concept of reverberation and apply a series of percolators and delay lines to mimic environmental space characteristics. There are two main methods for acquiring RIRs in the audio community [18, 46, 52]. **(1)** Simulation techniques can be employed to produce RIRs when the geometry and material properties of the spatial environment are available [2, 3, 16]. **(2)** If detailed information is inaccessible, RIRs can be blindly estimated from audio captured in the room [52, 71]. RIRs are then employed to synthesize an auralized audio signal. Both methods have weaknesses. The former requires exhaustive measurements of space that may be infeasible, while the latter may introduce some disturbances due to limited acoustic information. Some recent works [34, 68] attempt to approximate RIRs from an environmental image, necessitating paired image and impulse response training data. Regrettably, these methods also require estimating the acoustic parameters from the recorded audio, which severely limits the application scopes. Chen *et al.* [4] introduce VAM and utilize visual observation to simulate the target environment for generating reverberant audio. However, VAM focuses on acoustic matching, neglecting the correlation and inherent consistency with the reverse dereverberation task. In this paper, we harness the RGB image of specified environment for acoustic matching and utilize the reciprocity with dereverberation to improve the precision of reverberation simulations.

**Dereverberation.** Due to the challenge of collecting both anechoic and reverberant audio simultaneously, acoustic dereverberation can enhance training data quality by minimizing reverberation disturbance [33, 86]. The main stream dereverberation technologies utilize devices like microphone arrays to remove reverberation [51]. Deep learning techniques have also made great strides in reverberation removal [22, 81, 87]. Tan *et al.* [74] exploit the movement of the upper lip region to isolate interfering sounds, yet it does not intentionally eliminate reverberation based on visual scene understanding. These methods either disregard or only partially take into account visual information. Chen *et al.* [6] propose learning all the acoustics characteristics associated with indoor dereverberation. Like acoustic matching, these unidirectional approaches neglect the reciprocal relationship between the two tasks, leading to an incomplete utilization of naturally recorded audio. In contrast, MVSD demonstrates stronger dereverberation capabilities through the assistance of symmetric tasks.

**Mutual Learning.** Mutual learning, originating from the field of language translation, aims to reduce dependence on data annotation [23]. This mechanism allows alternating between the two sides and enables the language model

to train solely from one-sided data. The core idea of mutual learning involves establishing a dual-learning game between two agents, each agent is assigned an individual task. In the primal task, mutual learning maps  $\mathbf{x}$  from primal domain to dual domain  $\mathbf{y}$ , and then restore the original  $\mathbf{x}$  through the reverse mapping in dual task [77, 88]. Hence, mutual learning can produce two feedback signals without requiring parallel data: a style evaluation score indicating the likelihood that the synthesized audio matches the target style, and a reconstruction loss measuring the difference between the reconstructed audio and the original audio. This mechanism alternates between agents, allowing the generator to train from only one-way data [42, 66, 82, 84, 85, 88]. We are the first to investigate the duality of VAM and dereverberation. These two tasks are trained together in a mutual learning framework and provide mutual reinforcement signals based on the structural symmetry, even for unpaired samples.

**Condition-guided Generation.** In recent years, there have been significant advancements in the field of conditional generation [26, 59, 67, 78]. Diffusion models have demonstrated impressive results in various generative tasks due to their superior visual quality and training stability [1, 9, 10, 25, 35, 41, 43, 50, 56, 63]. The diffusion probability model [69] is based on a Markov chain, proceeding through finite steps in two opposing directions: one transition moves from the data distribution to noise, and the other transitions back from noise to the data distribution. Ho *et al.* [25] introduce the variational lower bound objective, which is subsequently improved in [56] to obtain higher log-likelihood scores. In this study, we regard audio spectrograms as images and elegantly employ two diffusion-based generators for controllable reverberation style transfer.

### 3 Methodology

We propose a mutual learning framework MVSD to leverage feedback signals from symmetrical tasks to promote model training and better exploit unpaired data. It involves two tasks: a primal task VAM [4] that employs the reverberator  $f_\theta$  to convert an anechoic audio  $\mathbf{a}_c$  into a reverberated audio  $\hat{\mathbf{a}}_r$ , which is aurally recorded in the specified environment. In the dual task, dereverberator  $g_\phi$  removes the reverberant characteristics in  $\mathbf{a}_r$ , which is similar to its anechoic counterpart  $\mathbf{a}_c$ . Here,  $f_\theta$  and  $g_\phi$  are jointly trained in an end-to-end mutual learning framework MVSD (§3.1). Furthermore, we employ visual scene-driven diffusion models as foundational conditional converters  $f_\theta$  and  $g_\phi$  to achieve stable training and accurate reverberation style transfer (§3.2).

**Reverberator.** Consider paired data distributions:  $\mathbf{A}_c = \{\mathbf{a}_c^{(1)}, \mathbf{a}_c^{(2)}, \dots, \mathbf{a}_c^{(n)}\}$  and  $\mathbf{A}_r = \{\mathbf{a}_r^{(1)}, \mathbf{a}_r^{(2)}, \dots, \mathbf{a}_r^{(n)}\}$ , representing anechoic and reverberant audio, respectively. The set of visual scenes  $\mathbf{V} = \{\mathbf{v}^{(1)}, \mathbf{v}^{(2)}, \dots, \mathbf{v}^{(n)}\}$  corresponds to the audio set of  $\mathbf{A}_r$ . The goal of VAM is to convert the anechoic audio  $\mathbf{a}_c$  with condition  $\mathbf{v}$  to its reverberant counterpart  $\mathbf{a}_r$ , *i.e.*, to estimate the conditional distribution  $f_\theta(\mathbf{a}_r|\mathbf{a}_c; \mathbf{v})$ . Based on diffusion models, we encode  $\mathbf{a}_c$  into content features and switch the reverberation style to the visual environment  $\mathbf{v}$ .

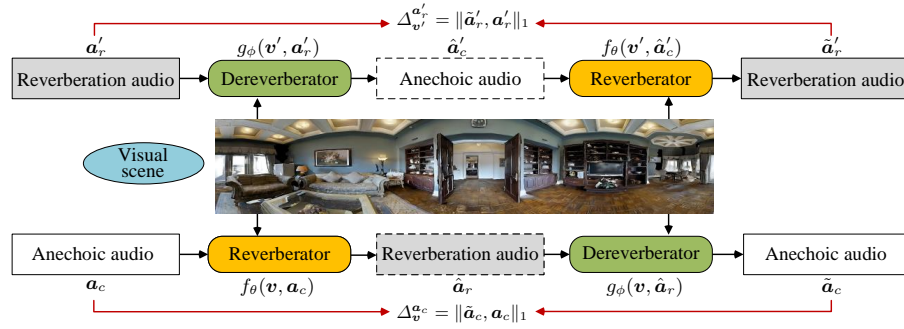


**Fig. 2:** The overview of MVSD. The output of a converter can serve as pseudo-input for the reverse task, providing an intermediate transition. Concretely, the reverberator  $f_\theta$  and dereverberator  $g_\phi$  can generate feedback signals  $\mathcal{L}_m$  (Eq. 4) for mutual optimization of training, even with one-way unpaired data  $(\mathbf{a}'_r, \mathbf{v}')$  (§3.1).

**Dereverberator.** Contrary to VAM, the goal of the dereverberation task is to eliminate reverberation factors and enhance the intelligibility of audio content. Correspondingly, the dereverberator  $g_\phi$  based on VSD calculates the anechoic distribution  $g_\phi(\mathbf{a}_c | \mathbf{a}_r; \mathbf{v})$  under a given scene  $\mathbf{v}$ .

### 3.1 Mutual Learning

We jointly learn the VAM and dereverberation tasks (Fig. 2): the reverberator  $f_\theta$  and dereverberator  $g_\phi$  can mutually benefit from each other. Suppose we have two (vanilla) converters that can map anechoic audio to a specified reverberation style and vice versa. Our goal is to simultaneously improve the style accuracy of the VAM task and the content intelligibility of the dereverberation task by employing paired and unidirectional non-paired data. To achieve this, we leverage the reciprocity between these two tasks, wherein the input-output spaces of VAM and dereverberation exhibit a strong correlation and can interchangeably act as the input and output for each other. Starting from either task, we first convert it forward to another audio, then transfer it backward to the original audio. By evaluating the results of this two-hop transfer process, we can gauge the quality of both converters and optimize them accordingly. Namely, dereverberator  $g_\phi$  is employed to evaluate the quality of  $\hat{\mathbf{a}}_r$  generated by  $f_\theta$  and sends back an error signal  $\Delta(\tilde{\mathbf{a}}_c, \mathbf{a}_c)$  to  $f_\theta$ , and vice versa. This process can be iterated many rounds until both converters converge. Please note that in MVSD,  $\mathbf{a}_r$  and  $\mathbf{a}_c$  are not necessarily aligned and may even not have a typical relationship.

We denote a labeled collection as  $\mathcal{D} = \{(\mathbf{v}^n, \mathbf{a}_c^n, \mathbf{a}_r^n)\}_{n=1}^N$ , which consists of  $N$  aligned tuples of anechoic and reverberant audio. Given a triplet  $\langle \mathbf{v}, \mathbf{a}_c, \mathbf{a}_r \rangle$ , where  $\mathbf{v}$ ,  $\mathbf{a}_c$ ,  $\mathbf{a}_r$  are sets of *environmental spaces*, *anechoic* and *target audios*. Our goal is to uncover the bi-directional relationship between the  $\mathbf{a}_c$  and  $\mathbf{a}_r$ . For the primal process starting from VAM, denote  $\hat{\mathbf{a}}_r$  as the mid-transition output. Firstly, we obtain a reverberated audio  $\hat{\mathbf{a}}_r$  through the reverberator  $f_\theta(\mathbf{v}, \mathbf{a}_c)$ . Then, the dereverberator  $g_\phi$  translates  $\hat{\mathbf{a}}_r$  to  $\tilde{\mathbf{a}}_c$  by mapping  $g_\phi(\mathbf{v}, \hat{\mathbf{a}}_r)$ . The  $\tilde{\mathbf{a}}_c$  is

expected to be consistent with  $\mathbf{a}_c$  in audio clarity, *i.e.*, achieving a small cycle-consistency error  $\Delta_{\mathbf{v}}^{\mathbf{a}_c}$ . Similarly, for dereverberator  $g_\phi$ , we have  $\tilde{\mathbf{a}}_r = f_\theta(\mathbf{v}, \hat{\mathbf{a}}_c)$  and  $\tilde{\mathbf{a}}_r$  should have a reverberation effect akin to  $\mathbf{a}_r$  in auditory perception. Likewise,  $\Delta_{\mathbf{v}}^{\mathbf{a}_r}$  can be employed to evaluate the discrepancies between  $\mathbf{a}_r$  and  $\tilde{\mathbf{a}}_r$ . Finally, the errors  $\Delta_{\mathbf{v}}^{\mathbf{a}_c}$  and  $\Delta_{\mathbf{v}}^{\mathbf{a}_r}$  can be specified as two reconstruction losses, which are minimized for the model training. Prior researches [23, 38] on conditional image synthesis suggest that  $L1$  distance, unlike  $L2$ , can reduce blurriness. Hence, we employ  $L1$  distance to assess the feedback errors:

$$\begin{aligned}\Delta_{\mathbf{v}}^{\mathbf{a}_r} &= \|\tilde{\mathbf{a}}_r, \mathbf{a}_r\|_1 = \|f_\theta(\mathbf{v}, g_\phi(\mathbf{v}, \mathbf{a}_r)) - \mathbf{a}_r\|_1; \\ \Delta_{\mathbf{v}}^{\mathbf{a}_c} &= \|\tilde{\mathbf{a}}_c, \mathbf{a}_c\|_1 = \|g_\phi(\mathbf{v}, f_\theta(\mathbf{v}, \mathbf{a}_c)) - \mathbf{a}_c\|_1.\end{aligned}\quad (1)$$

In real-world scenarios, the challenge of capturing parallel data arises from the difficulty of simultaneously recording sound at the source and listener locations. This obstacle is mitigated in our approach, as it does not necessitate aligned anechoic and reverberant pairs  $(\mathbf{a}_c, \mathbf{a}_r)$  for the errors  $\Delta_{\mathbf{v}}^{\mathbf{a}_r}$  and  $\Delta_{\mathbf{v}}^{\mathbf{a}_c}$ . As a result, Eq. 1 can be effectively applied to one-way unpaired audios. As in common practice [13, 29, 73], we build two unlabeled collections:  $\mathcal{U} = \{(\mathbf{v}^{m'}, \mathbf{a}_r^{m'})\}_{m=1}^M$  for audios with natural reverberation, and  $\mathcal{C} = \{\mathbf{a}_c^{k''}\}_{k=1}^K$  with only anechoic audio. We obtain  $\mathcal{U}$  by sampling natural audios  $\mathbf{a}'_r$  from existing environments  $\mathbf{v}'$ , which lack corresponding anechoic audios. Similarly, we create collection  $\mathcal{C}$  by filtering anechoic audios [6]  $\mathbf{a}''_c$  from an open-source dataset [58], which do not have matching reverberated audios and visual images. For unpaired natural audios  $\mathcal{U}$ , we first generate intermediate output  $\hat{\mathbf{a}}'_c$  using the dereverberator  $f_\theta(\mathbf{a}'_r, \mathbf{v}')$ , followed by reconstructing  $\tilde{\mathbf{a}}'_r$  based on  $\hat{\mathbf{a}}'_c$  and scene  $\mathbf{v}'$ , *i.e.*,  $g_\phi(\mathbf{v}', \hat{\mathbf{a}}'_c)$ , and computing error  $\Delta_{\mathbf{v}'}^{\mathbf{a}'_r}$  against the original input  $\mathbf{a}'_r$ . We can derive the formula:

$$\Delta_{\mathbf{v}'}^{\mathbf{a}'_r} = \|\tilde{\mathbf{a}}'_r, \mathbf{a}'_r\|_1 = \|f_\theta(\mathbf{v}', g_\phi(\mathbf{v}', \mathbf{a}'_r)) - \mathbf{a}'_r\|_1. \quad (2)$$

As for unpaired anechoic audios  $\mathcal{C}$ , since there are rarely accompanying visual scene images when recording audio, we randomly sample an image  $\mathbf{v}''$  from  $\mathcal{U}$  to simulate the specified environment, and the formulate is as:

$$\Delta_{\mathbf{v}''}^{\mathbf{a}''_c} = \|\tilde{\mathbf{a}}''_c, \mathbf{a}''_c\|_1 = \|g_\phi(\mathbf{v}'', f_\theta(\mathbf{v}'', \mathbf{a}''_c)) - \mathbf{a}''_c\|_1. \quad (3)$$

Our training process utilizes paired data, complemented by unpaired natural and anechoic audios. Consequently, our mutual learning loss is defined as:

$$\mathcal{L}_m = \frac{1}{N} \sum_{(\mathbf{v}, \mathbf{a}_r, \mathbf{a}_c) \in \mathcal{D}} (\Delta_{\mathbf{v}}^{\mathbf{a}_c} + \Delta_{\mathbf{v}}^{\mathbf{a}_r}) + \frac{1}{M} \sum_{(\mathbf{v}', \mathbf{a}'_r) \in \mathcal{U}} \Delta_{\mathbf{v}'}^{\mathbf{a}'_r} + \frac{1}{K} \sum_{(\mathbf{v}'', \mathbf{a}''_c) \in \mathcal{C}} \Delta_{\mathbf{v}''}^{\mathbf{a}''_c}. \quad (4)$$

During training,  $\mathcal{L}_m$  is applied only for predictions and backpropagation at time step  $t$  of the diffusion model. Hence, MVSD does not significantly increase the training time compared to training the two tasks separately.

**Remark.** MVSD consists of two main concepts: First, an ideal reverberator should be able to adapt audio to any visual environment, and a dereverberator is also effective at removing disturbances that affect speech intelligibility. Therefore, we investigate VAM and dereverberation in a unified learning framework,

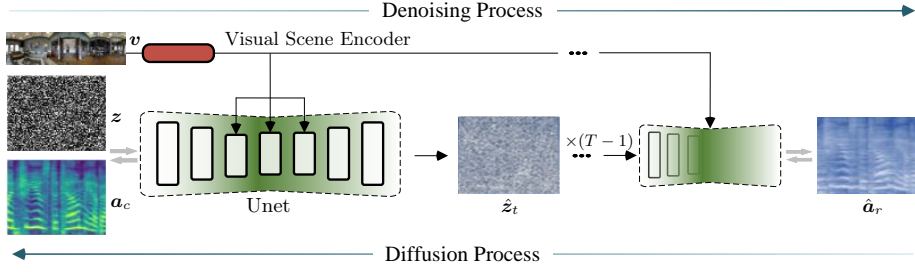


**Fig. 3:** The diffusion and denoising processes of VSD. Taking VAM as an example, MVSD converts anechoic audio  $\mathbf{a}_c$  into reverberant audio  $\hat{\mathbf{a}}_r$  that aligns with the acoustics of the visual scene  $\mathbf{v}$  (§3.2).

allowing the converters to better exploit the cross-modal and cross-task correlations. Second, the addition of unpaired data can boost model performance, and paired data guides the reverberator and dereverberator converge to the target distribution, preventing extreme domain deviation from the unpaired data.

### 3.2 Visual Scene-driven Diffusion

In MVSD, the reverberator and dereverberator share a similar model structure. We introduce visual scene-driven diffusion (VSD) with the reverberator  $f_\theta$  as an example. The diffusion model employs a  $T$ -step iterative denoising process to transform Gaussian noise into the desired data distribution [25, 63, 69]. By introducing prompt conditions such as class labels and text [10, 57], the generated content can be controlled precisely. In MVSD, visual scene embeddings are employed as control conditions to guide the generation of reverberator  $f_\theta$  and dereverberator  $g_\phi$ . In particular, the diffusion process follows a Markov chain, progressively adding noise to the input spectrogram  $\mathbf{x}_0$  (sampled from the real distribution  $q(\mathbf{x})$ ) until it evolves into white Gaussian noise  $\mathcal{N}(0, 1)$ . At each step  $t$ , the spectrogram  $\mathbf{x}_t$ , following the distribution  $q(\mathbf{x}_t|\mathbf{x}_{t-1})$ , is derived by the pre-defined variance  $\beta_t$  scaled with  $\sqrt{1 - \beta_t}$ :

$$q(\mathbf{x}_t|\mathbf{x}_{t-1}) = \mathcal{N}(\mathbf{x}_t; \mathbf{z}_t); \quad \mathbf{z}_t \sim \mathcal{N}(\sqrt{1 - \beta_t}\mathbf{z}_{t-1}, \beta_t\mathbf{I}). \quad (5)$$

The denoising process attempts to restore the original spectrogram  $\mathbf{x}_0$  from the noisy data  $\mathbf{x}_T$  by removing the noise introduced in the forward diffusion process. The prediction  $q(\mathbf{x}_{t-1}|\mathbf{x}_t)$  at step  $t - 1$  is approximated by a parameterized model  $p$  (e.g., a neural network), involving the estimation of  $\mu(\mathbf{z}_t, t)$  and  $\sigma(\mathbf{z}_t, t)$  from a Gaussian distribution. By employing the reverse process across all time steps, we can transition from  $\mathbf{x}_T$  back to the initial spectrogram  $\mathbf{x}_0$ :

$$\begin{aligned} p(\mathbf{x}_{0:T}) &= p(\mathbf{x}_T) \prod_{t=1}^T p(\mathbf{x}_{t-1}|\mathbf{x}_t) \\ &= p(\mathbf{x}_T) \prod_{t=1}^T \mathcal{N}(\mathbf{x}_{t-1}; \mu(\mathbf{x}_t, t), \sigma(\mathbf{x}_t, t)). \end{aligned} \quad (6)$$

**Visual Scene Encoder.** We apply an embedding with 256 dimensions to represent visual scenes, extracted by a pre-trained ResNet-18 [24] encoder. Then, the embedding serves as the condition to guide the generation of diffusion models.

**Controllable Unet.** We meticulously design an controllable Unet for predicting  $\mathbf{x}_t$  of diffusion (Fig. 3). Controllable Unet is composed of multiple stages with attention blocks [63], *i.e.*, self-attention and cross-attention. Self-attention allows a model to weigh the importance of different parts within the same element. Cross-attention, similar to self-attention, targets relationships across different components. We employ a classic encoder-decoder with a symmetric design, where each part incorporating 3 attention blocks. The encoder progressively reduces the resolution of the feature map, and then the decoder gradually increases it to align with the size of the original spectrogram. In the self-attention block, we utilize the downsampling method in [72] with a stride of 4 to rapidly decrease the size of feature maps. The downsampling utilizes dilated convolutions and attention to increase the receptive field without reducing spatial dimensions. Cross-modal attention is selectively employed to the third encoder block and the first decoder block, mitigating computational overhead. Both VAM and dereverberation need to preserve the linguistic information in the audios. Therefore, we concatenate source spectrogram with the noise  $\mathbf{z}_0$  as the content input for the controllable Unet. Please refer to the supplementary material for details.

### 3.3 Training Objective

For training the diffusion model, we employ the simplified objective [25]:

$$\mathcal{L}_d = \mathbb{E}_{\mathbf{x}_0, t, \mathbf{z}} [\|\mathbf{z} - \hat{\mathbf{z}}(\sqrt{\alpha_t}\mathbf{x}_0 + \sqrt{1 - \alpha_t}\mathbf{z}, t)\|_2], \quad (7)$$

where  $\alpha_t$  in diffusion models is a scaling factor that modulates the noise level at each time step  $t$ . VSD can predict the noise  $\hat{\mathbf{z}}_t$  and use it to iteratively refine the denoising process. With the reparameterization trick, a method for differentiable sampling [32], we can represent the estimation of  $\hat{\mathbf{x}}_0$ :

$$\hat{\mathbf{x}}_0 = \frac{1}{\sqrt{\alpha_t}}(\mathbf{x}_t - \sqrt{1 - \alpha_t}\hat{\mathbf{z}}_t). \quad (8)$$

Moreover, we introduce a style loss  $\mathcal{L}_{sty}$  (Eq. 9) to make the generated audios with the environmental characteristics. Taking VAM task as an example, during training, the Unet predicts the noise  $\hat{\mathbf{z}}_t$  at time step  $t$ . Then,  $\hat{\mathbf{z}}_t$  can be used to gradually derive the predicted original spectrogram  $\hat{\mathbf{x}}_r$  at step 0 (Eq. 8). Here, we do not explicitly extract the stylistic features of the  $\mathbf{a}_r$  and  $\hat{\mathbf{a}}_r$ ; instead, we directly employ  $\mathcal{L}_1$  loss to regularize style consistency:

$$\mathcal{L}_{sty} = \|\hat{\mathbf{a}}_r - \mathbf{a}_r\|_1 + \|\hat{\mathbf{a}}_c - \mathbf{a}_c\|_1. \quad (9)$$

We learn models  $f_\theta$  and  $g_\phi$  by minimizing the combination of the diffusion loss, the style loss and the mutual learning regularization term. In summary, the overall training objective is given as:

$$\mathcal{L}_{total} = \mathcal{L}_d + \mathcal{L}_m + \mathcal{L}_{sty}. \quad (10)$$

### 3.4 Implementation Details

**Training.** In MVSD, converters and visual scene encoder are trained separately. We adopt the loss function in [30] to train the visual scene encoder. The mutual learning is integrated into each mini-batch update, spanning the entire training process for the two tasks. Training starts with supervised data, with unsupervised data progressively merged for optimization. This stepwise strategy can preserve model stability. At each iteration, we compute the predictions of both converters and update their parameters based on the feedback from the symmetrical models. In practice, we first perform supervised training and conduct the loop of mutual learning (Alg. 1). Besides minimizing the cycle-consistent loss  $\mathcal{L}_m$  (Eq. 4), our MVSD framework is learnt with the diffusion objectives for VAM and dereverberation, over the labeled data  $\mathcal{D}$ . Finally, we receive a prepared model when MVSD converges on all training data.

---

**Algorithm 1:** Mutual learning with visual scene-driven diffusion.

---

- Input:** Labeled set  $\mathcal{D}$ , unpaired sets  $\mathcal{U}$  and  $\mathcal{C}$ , reverberator  $f_\theta$  and dereverberator  $g_\phi$ .
- 1 **Repeat:** Sample a mini-batch of paired tuples  $\langle \mathbf{a}_c, \mathbf{v}, \mathbf{a}_r \rangle$ ;
  - 2 Generate random Gaussian noise  $\mathbf{z}_c$  and  $\mathbf{z}_r$  for the converters;
  - 3 Execute the diffusion processes of reverberator  $f_\theta$  and dereverberator  $g_\phi$ ;
  - 4 Calculate the training objective  $\mathcal{L}_{total}$  (Eq. 10);
  - 5 Update the parameters of  $\theta$  and  $\phi$ :  $\theta \leftarrow \theta - \gamma \nabla_\theta \mathcal{L}(\theta)$ ,  $\phi \leftarrow \phi - \gamma \nabla_\phi \mathcal{L}(\phi)$ ;
  - 6 Introduce unpaired data and continue training when the epoch exceeds 100;
  - 7 **Until:** Convergence
- 

**Inference.** The inference of each task follows the sampling process of the diffusion model. Take VAM as an example: First, a noise spectrogram is randomly generated and concatenated with an anechoic test spectrogram. Next, at each step  $t$  of the denoising process, the controllable Unet synthesizes the intermediate spectrogram conditioned on visual features. We report the average of ten experiments as the evaluation criterions.

**Reproductibility.** Our model is implemented in PyTorch and trained using two NVIDIA Tesla V100 GPUs. Training MVSD from scratch takes approximately 144 hours. The average inference time is 1.09 seconds. We set FFT size, hop size and mel scale for audio processing to 1024, 256 and 128, respectively. We then truncate the mel-spectrogram to a width of 128, resulting in a spectrogram size of  $128 \times 128$ . We utilize a pre-trained BigVGAN [39] as the vocoder.

## 4 Experiments

**Dataset.** We conduct experiments on two datasets [4]: *SoundSpaces-Speech* and *Acoustic AVSpeech* datasets. The former employs a simulated environment [5] to generate reverberation audio, is perfectly aligned paired audio and accurate ground truth. Regardless, there has a realism gap. Finally, the dataset is split into

**Table 1:** Quantitative results on *SoundSpaces-Speech* and *Acoustic AVSpeech* [4] (§4.1).

Method	<i>SoundSpaces-Speech</i>						<i>Acoustic AVSpeech</i>			
	<i>Seen</i>			<i>Unseen</i>			<i>Seen</i>		<i>Unseen</i>	
	STFT ↓	RTE (s) ↓	MOSE ↓	STFT ↓	RTE (s) ↓	MOSE ↓	RTE (s) ↓	MOSE ↓	RTE (s) ↓	MOSE ↓
Input audio	1.192	0.331	0.617	1.206	0.356	0.611	0.387	0.658	0.392	0.634
AEE [71]	2.746	0.319	0.571	-	-	-	-	-	-	-
Image2Reverb [68]	2.538	0.293	0.508	2.318	0.317	0.518	-	-	-	-
AV U-Net [19]	0.638	0.095	0.353	0.658	0.118	0.367	0.156	0.570	0.188	0.540
AViTAR [4]	0.665	0.034	0.161	0.822	0.062	0.195	0.144	0.481	0.183	0.453
MVSD <i>w/o</i> visual scene	0.691	0.188	0.156	0.803	0.155	0.194	0.137	0.526	0.171	0.474
MVSD <i>w/o</i> unpaired data	0.573	0.033	0.148	0.736	0.055	0.184	0.131	0.427	0.159	0.394
<b>MVSD</b>	<b>0.508</b>	<b>0.030</b>	<b>0.142</b>	<b>0.637</b>	<b>0.051</b>	<b>0.178</b>	<b>0.112</b>	<b>0.392</b>	<b>0.148</b>	<b>0.379</b>

*train/val/test* sets with 28, 853, 1, 441, and 1, 489 samples, respectively. Acoustic AVSpeech is a subset of AVSpeech dataset [11]. It offers more realism but poses evaluation challenges due to lacking corresponding reverberant audios. Acoustic AVSpeech contains 113k/3k/3k video clips for the training, validation, and test splits, respectively. For the unpaired data, we randomly sample 5,000 natural audios with video in AVSpeech dataset [11] and 5k anechoic audio in LibriSpeech [58], with no overlap with the training sets. We apply ‘Seen’ and ‘Unseen’ to denote whether visual scenes are encountered during training.

**Evaluation Metrics.** For VAM task, following [4], we employ STFT-distance to measure deviation from the ground truth, Reverberation Time 60 error (RTE) for room acoustics, and Mean Opinion Score Error (MOSE) for speech quality evaluation. For dereverberation task, as in [6], we adopt Perceptual Evaluation of Speech Quality (PESQ) [62], Word Error Rate (WER) and Equal Error Rate (EER) to assess the aspects of audio quality, content precision, and speaker verification error, respectively. The evaluation is conducted on the anechoic version of LibriSpeech test set [6, 58].

#### 4.1 Performance on VAM

As shown in Table 1, MVSD achieves a notable absolute boost of 0.157 STFT-distance (23.6% relative improvement), 0.004 RTE (11.8% relative improvement), and 0.019 MOSE (11.8% relative improvement) in the ‘Seen’ split of SoundSpaces-Speech dataset compared with SOTA method. There is also a similar improvement in Acoustic AVSpeech dataset. We can see that MVSD exhibits outstanding strengths in all three assessed aspects: preserving source audio content better, getting in more precise signal attenuation and more consistent quality with the target audio. MVSD has the capability to infer and extract relevant factors that influence reverberation from target images, even in never-before-seen scenes. It should be noted that blind reverberator [71], a traditional acoustic method, needs reference audio, making it unsuitable for scenarios ‘Unseen’ of SoundSpaces (no reference audio) and AVSpeech, as reported in [4]. Fig. 4 showcases the visual comparisons of different methods for the VAM task on the SoundSpaces-Speech and AVSpeech datasets, respectively, highlighting the superiority of MVSD.

**Table 2:** Quantitative dereverberation results on SoundSpaces-Speech [4] (§4.2).

	Speech Enhancement PESQ $\uparrow$	Speech Recognition WER(%) $\downarrow$	Speaker Verification EER(%) $\downarrow$
Anechoic (Ceiling)	4.64	2.50	1.89
Reverberant	1.54	8.86	5.23
MetricGAN+ [15]	2.33	7.49	5.16
VIDA [6]	2.37	4.44	4.58
<b>MVSD</b>	<b>2.53</b>	<b>4.27</b>	<b>4.46</b>

**Table 3:** User study results. X%/Y% means that X% of participants prefer this method while Y% prefer MVSD (§4.3).

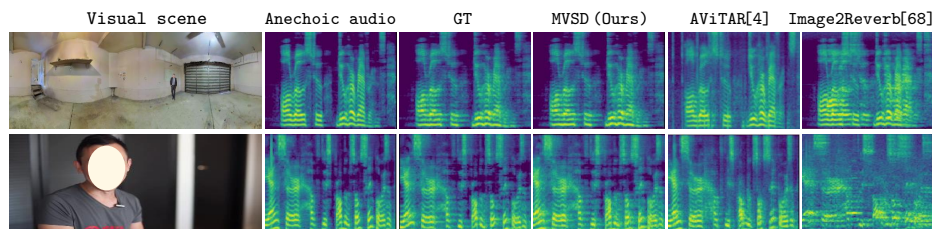
	SoundSpaces	AVSpeech
Input Speech	39.3% / <b>60.7%</b>	38.2% / <b>61.8%</b>
Image2Reverb [68]	20.8% / <b>79.2%</b>	- / -
AV U-Net [19]	23.4% / <b>76.6%</b>	21.9% / <b>78.1%</b>
AViTAR [4]	34.7% / <b>65.3%</b>	44.1% / <b>55.9%</b>

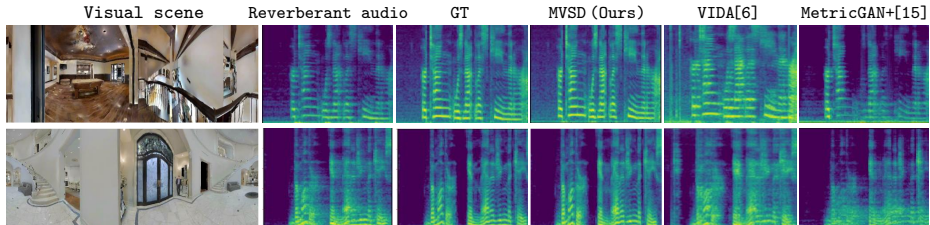
## 4.2 Performance on Derreverberation

Table 2 presents the dereverberation performance of MVSD on SoundSpaces-Speech [4] dataset. We observe that MVSD also demonstrates superior performance across all three metrics in the dereverberation task. Particularly in terms of WER, MVSD exhibits a remarkable error reduction of 0.17 compared to VIDA, achieving a value of 4.27%. This highlights the robust dereverberation capability of MVSD. Additionally, MVSD achieves an EER of 4.46%, demonstrating its ability to mitigate reverberation while preserving the timbre information. Fig. 5 depicts the spectrograms for the dereverberation task on SoundSpaces-Speech, with AVSpeech dataset omitted due to the absence of groundtruth anechoic audio. Spectrogram analysis reveals that MVSD achieves superior clarity and noise reduction in dereverberation, with distinct peaks and fewer artifacts. The improvements observed in both tasks signify that MVSD can leverage the reciprocity to enhance the learning capability.

## 4.3 User Study

The human ear is the most accurate tool for evaluating acoustic experiences. Therefore, we conduct a user study as a complement to quantitative indicators. We invited 15 volunteers to participate in the evaluation. Following the configuration in [4], we show participants some images of the target environment, real audio clips, and samples generated by all test methods. Participants is asked to choose the audio sample that exhibit the highest consistency with

**Fig. 4:** Visualization results for VAM task on the SoundSpaces-Speech (top) and AVSpeech datasets (bottom) [4] (§4.1).



**Fig. 5:** Visualization of the dereverberation task on the SoundSpaces-Speech [4] (§4.2).

the groundtruth reverb style and 30 samples are selected for each dataset. Table 3 reports the final preference scores. As expected, MVSD consistently exceeds the results of other methods, achieving a high preference ratio against AVITAR [4] (65.3% in SoundSpaces and 55.9% in AVSpeech). A certain percentage (39.3% and 38.2%) of subjects prefer ‘clean’ audio devoid of reverberation, which can be seen from the first row of Table 3. This tendency can be attributed to the general preference for ‘clean’ sounding audio among those participants without professional acoustical knowledge, which is also reported in [4].

#### 4.4 Ablation Study

To assess the effectiveness of MVSD’s key components, we conduct diagnostic studies and report VAM results on SoundSpaces-Speech dataset [4] and using WER and PESQ metrics for dereverberation.

**Mutual Learning.** We conduct three diagnostic experiments: i) VSD – training two tasks separately with the structure akin to mutual learning; ii) MVSD *w/o* unpaired data – training exclusively with labeled data; and iii) MVSD – augmenting the second experiment with unpaired data. Table 4a reveals that our baseline model VSD can achieve performance matching SOTA on metrics STFT 0.657 and MOSE 0.159. The introduction of MVSD results in a slight edge over SOTA, and incorporating unpaired data notably surpasses SOTA in both tasks (achieved 0.508 STFT, 0.030 RTE, 0.142 MOSE in VAM, and 4.27% WER, 2.53 PESQ in dereverberation, respectively). These findings highlight that the synergy between dual tasks can enhance learning capabilities and efficiently absorb unpaired data, showcasing the benefit of a wealth of natural data.

**Model Design.** To validate the superiority of diffusion model, we conduct comparative experiments with two different generator architectures: (1) a conditional generative network based on GAN, influenced by our single-task model, and (2) The controllable Unet in MVSD, designed to showcase the diffusion process. Table 4b shows the controllable Unet outperforms the GAN-based model significantly in all evaluated metrics, STFT reduced by 0.078 to 0.753. WER decreased by 1.57% to 6.74%. The diffusion process significantly further enhances the performance to achieve 0.657 STFT and 4.27% WER. Compared to GANs, diffusion models can excel in stability and sample quality, enabling a more controllable and precise generation process.

**Table 4:** A series of ablation studies on SoundSpaces-Speech dataset [4] (§4.4).

Method	VAM			Dereverberation	
	STFT ↓	RTE(s) ↓	MOSE ↓	WER ↓	PESQ ↑
VSD	0.657	0.037	0.159	4.39	2.41
MVSD <i>w/o</i> unpaired data	0.573	0.033	0.148	4.32	2.47
<b>MVSD</b>	<b>0.508</b>	<b>0.030</b>	<b>0.142</b>	<b>4.27</b>	<b>2.53</b>

(a) mutual learning

Method	VAM			Dereverberation	
	STFT ↓	RTE(s) ↓	MOSE ↓	WER ↓	PESQ ↑
CNN-GAN	0.831	0.076	0.237	8.31	1.93
Unet <i>w/o</i> diffusion	0.753	0.067	0.194	6.74	2.19
<b>Diffusion</b>	<b>0.657</b>	<b>0.037</b>	<b>0.159</b>	<b>4.27</b>	<b>2.53</b>

(b) diffusion model

Steps	VAM			Dereverberation		Timeliness RTF ↑
	STFT ↓	RTE(s) ↓	MOSE ↓	WER ↓	PESQ ↑	
150	1.452	0.242	0.376	8.39	1.48	<b>0.253</b>
250	0.508	0.030	0.142	4.27	2.53	0.426
350	0.493	0.035	<b>0.139</b>	<b>4.26</b>	2.47	0.619
500	0.492	<b>0.029</b>	0.144	4.28	<b>2.55</b>	0.898
1000	<b>0.487</b>	0.033	0.141	4.35	2.49	1.809

(c) denoising steps

Num	VAM			Dereverberation	
	STFT ↓	RTE(s) ↓	MOSE ↓	WER ↓	PESQ ↑
0 <i>k</i>	0.573	0.033	0.148	4.32	2.47
1 <i>k</i>	0.547(+4.5%)	0.033(+0.0%)	0.147(+0.7%)	4.28	2.50
3 <i>k</i>	0.521(+9.1%)	0.031(+6.1%)	0.143(+3.4%)	4.29	2.52
5 <i>k</i>	<b>0.508(+11.3%)</b>	<b>0.030(+9.1%)</b>	<b>0.142(+4.1%)</b>	<b>4.27</b>	<b>2.53</b>

(d) unpaired data size

**Denoising Steps.** We conduct experiments varying the number of denoising steps, as detailed in Table 4c and apply the Real-Time Factor (RTF) to measure the speed of audio generation relative to the actual duration of the audio. Results indicate suboptimal generation for steps under 250. At 250 steps, MVSD matches SOTA performance. However, more steps require longer training time but yield minimal improvement, increasing the runtime by at least 30%. Consequently, we establish 250 as the optimal number of diffusion steps.

**Unpaired Data Size.** We diagnose the impact of unlabeled data by investigating the correlation between the quantity of unpaired data and performance. As shown in Table 4d, increasing the amount of unpaired data consistently boosts the performance. Incorporating unpaired data equivalent to 17.3% of the supervised samples, STFT-distance shows a notable improvement of 11.3%. Similar conclusions can also be observed in the dereverberation results. More unpaired data enables the model to learn from a broader data distribution, improving its predictive accuracy and stability.

## 5 Conclusion

In this paper, we introduce MVSD, a mutual learning framework based on visual scene-driven diffusion model, designed for VAM and dereverberation tasks. In early exploration, we combine diffusion model with mutual learning, a strategy that leverages the complementary aspects between tasks to improve both the performance and the generalization capabilities. Consequently, MVSD achieves SOTA performance in the both tasks. We empirically demonstrate that by utilizing a symmetric diffusion model architecture, MVSD can effectively extract and utilize cross-task knowledge across both tasks. Furthermore, by integrating an additional 17.3% of unpaired data into the training set, we have observed a 9.1% relative improvement in RTE for VAM. This strategy allows MVSD to access easily acquired unpaired data, thereby reducing the reliance on annotation. We anticipate our research will enhance the utilization of unidirectional data.

## References

1. Avrahami, O., Lischinski, D., Fried, O.: Blended diffusion for text-driven editing of natural images. In: CVPR (2022)
2. Bilbao, S.: Modeling of complex geometries and boundary conditions in finite difference/finite volume time domain room acoustics simulation. *IEEE Trans. Audio Speech Lang. Process.* **21**(7), 1524–1533 (2013)
3. Cao, C., Ren, Z., Schissler, C., Manocha, D., Zhou, K.: Interactive sound propagation with bidirectional path tracing. *ACM Trans. Graph.* **35**(6), 1–11 (2016)
4. Chen, C., Gao, R., Calamia, P., Grauman, K.: Visual acoustic matching. In: CVPR (2022)
5. Chen, C., Jain, U., Schissler, C., Gari, S.V.A., Al-Halah, Z., Ithapu, V.K., Robinson, P., Grauman, K.: Soundspaces: Audio-visual navigation in 3d environments. In: ECCV (2020)
6. Chen, C., Sun, W., Harwath, D., Grauman, K.: Learning audio-visual dereverberation. In: ICASSP (2023)
7. Chen, J., Wang, W., Liu, S., Li, H., Yang, Y.: Omnidirectional information gathering for knowledge transfer-based audio-visual navigation. In: ICCV (2023)
8. Chen, X., Duan, Y., Houthoofd, R., Schulman, J., Sutskever, I., Abbeel, P.: Infogan: Interpretable representation learning by information maximizing generative adversarial nets. In: NeurIPS (2016)
9. Choi, J., Kim, S., Jeong, Y., Gwon, Y., Yoon, S.: ILVR: conditioning method for denoising diffusion probabilistic models. In: ICCV (2021)
10. Dhariwal, P., Nichol, A.: Diffusion models beat gans on image synthesis. In: NeurIPS (2021)
11. Ephrat, A., Mosseri, I., Lang, O., Dekel, T., Wilson, K., Hassidim, A., Freeman, W.T., Rubinstein, M.: Looking to listen at the cocktail party: A speaker-independent audio-visual model for speech separation. In: SIGGRAPH (2018)
12. Ernst, O., Chazan, S.E., Gannot, S., Goldberger, J.: Speech dereverberation using fully convolutional networks. In: EUSIPCO (2018)
13. Fried, D., Hu, R., Cirik, V., Rohrbach, A., Andreas, J., Morency, L.P., Berg-Kirkpatrick, T., Saenko, K., Klein, D., Darrell, T.: Speaker-follower models for vision-and-language navigation. In: NeurIPS (2018)
14. Fu, S.W., Liao, C.F., Tsao, Y., Lin, S.D.: Metricgan: Generative adversarial networks based black-box metric scores optimization for speech enhancement. In: ICML (2019)
15. Fu, S., Yu, C., Hsieh, T., Plantinga, P., Ravanelli, M., Lu, X., Tsao, Y.: Metricgan+: An improved version of metricgan for speech enhancement. In: Interspeech (2021)
16. Funkhouser, T., Tsingos, N., Carlbom, I., Elko, G., Sondhi, M., West, J.E., Pingali, G., Min, P., Ngan, A.: A beam tracing method for interactive architectural acoustics. *The Journal of the acoustical society of America* **115**(2), 739–756 (2004)
17. Gade, A.C.: Acoustics in halls for speech and music. *Springer handbook of acoustics* pp. 317–366 (2014)
18. Gamper, H., Tashev, I.J.: Blind reverberation time estimation using a convolutional neural network. In: IWAENC (2018)
19. Gao, R., Grauman, K.: 2.5d visual sound. In: CVPR 2019
20. Goodfellow, I.J., Pouget-Abadie, J., Mirza, M., Xu, B., Warde-Farley, D., Ozair, S., Courville, A.C., Bengio, Y.: Generative adversarial nets. In: NeurIPS (2014)
21. Han, K., Wang, Y., Wang, D., Woods, W.S., Merks, I., Zhang, T.: Learning spectral mapping for speech dereverberation and denoising. *IEEE Trans. Audio Speech Lang. Process.* **23**(6), 982–992 (2015)

22. Han, K., Wang, Y., Wang, D., Woods, W.S., Merks, I., Zhang, T.: Learning spectral mapping for speech dereverberation and denoising. *IEEE Trans. Audio Speech Lang. Process.* **23**(6), 982–992 (2015)
23. He, D., Xia, Y., Qin, T., Wang, L., Yu, N., Liu, T., Ma, W.: Dual learning for machine translation. In: *NeurIPS* (2016)
24. He, K., Zhang, X., Ren, S., Sun, J.: Deep residual learning for image recognition. In: *CVPR* (2016)
25. Ho, J., Jain, A., Abbeel, P.: Denoising diffusion probabilistic models. In: *NeurIPS* (2020)
26. Hu, R., Singh, A.: Unit: Multimodal multitask learning with a unified transformer. In: *ICCV* (2021)
27. Karras, T., Aila, T., Laine, S., Lehtinen, J.: Progressive growing of gans for improved quality, stability, and variation. In: *ICLR* (2018)
28. Karras, T., Laine, S., Aila, T.: A style-based generator architecture for generative adversarial networks. In: *CVPR* (2019)
29. Ke, L., Li, X., Bisk, Y., Holtzman, A., Gan, Z., Liu, J., Gao, J., Choi, Y., Srini-vasa, S.: Tactical rewind: Self-correction via backtracking in vision-and-language navigation. In: *CVPR* (2019)
30. Khosla, P., Teterwak, P., Wang, C., Sarna, A., Tian, Y., Isola, P., Maschinot, A., Liu, C., Krishnan, D.: Supervised contrastive learning. In: *NeurIPS* (2020)
31. Kim, J., Gopakumar, M., Choi, S., Peng, Y., Lopes, W., Wetzstein, G.: Holographic glasses for virtual reality. In: *SIGGRAPH* (2022)
32. Kingma, D.P., Welling, M.: Auto-encoding variational bayes. In: *ICLR* (2014)
33. Ko, T., Peddinti, V., Povey, D., Seltzer, M.L., Khudanpur, S.: A study on data augmentation of reverberant speech for robust speech recognition. In: *ICASSP* (2017)
34. Kon, H., Koike, H.: Estimation of late reverberation characteristics from a single two-dimensional environmental image using convolutional neural networks. *Journal of the Audio Engineering Society* **67**(7/8), 540–548 (2019)
35. Kong, Z., Ping, W., Huang, J., Zhao, K., Catanzaro, B.: Diffwave: A versatile diffusion model for audio synthesis. In: *ICLR* (2021)
36. Kressner, A.A., Westermann, A., Buchholz, J.M.: The impact of reverberation on speech intelligibility in cochlear implant recipients. *The Journal of the Acoustical Society of America* **144**(2), 1113–1122 (2018)
37. Kuttruff, H., Mommertz, E.: Room acoustics. In: *Handbook of engineering acoustics*, pp. 239–267. London, U.K.: Springer (2012)
38. Larsen, A.B.L., Sønderby, S.K., Larochelle, H., Winther, O.: Autoencoding beyond pixels using a learned similarity metric. In: *ICML* (2016)
39. Lee, S., Ping, W., Ginsburg, B., Catanzaro, B., Yoon, S.: Bigvgan: A universal neural vocoder with large-scale training. In: *ICLR* (2023)
40. Li, K., Yang, Z., Chen, L., Yang, Y., Xiao, J.: Catr: Combinatorial-dependence audio-queried transformer for audio-visual video segmentation. In: *ACM MM* (2023)
41. Liu, X., Park, D.H., Azadi, S., Zhang, G., Chopikyan, A., Hu, Y., Shi, H., Rohrbach, A., Darrell, T.: More control for free! image synthesis with semantic diffusion guidance. In: *WACV* (2023)
42. Lu, J., Kannan, A., Yang, J., Parikh, D., Batra, D.: Best of both worlds: Transferring knowledge from discriminative learning to a generative visual dialog model. In: *NeurIPS* (2017)
43. Lugmayr, A., Danelljan, M., Romero, A., Yu, F., Timofte, R., Gool, L.V.: Repaint: Inpainting using denoising diffusion probabilistic models. In: *CVPR* (2022)

44. Luo, S., Tan, Y., Huang, L., Li, J., Zhao, H.: Latent consistency models: Synthesizing high-resolution images with few-step inference. CoRR **abs/2310.04378** (2023)
45. Ma, J., Wang, W., Yang, Y., Zheng, F.: Ms2sl: Multimodal spoken data-driven continuous sign language production. In: ACL (2024)
46. Mack, W., Deng, S., Habets, E.A.P.: Single-channel blind direct-to-reverberation ratio estimation using masking. In: Interspeech (2020)
47. Malpica, S., Serrano, A., Guerrero-Viu, J., Martin, D., Bernal, E., Gutierrez, D., Masiá, B.: Auditory stimuli degrade visual performance in virtual reality. In: SIGGRAPH (2022)
48. Meng, C., He, Y., Song, Y., Song, J., Wu, J., Zhu, J., Ermon, S.: Sdedit: Guided image synthesis and editing with stochastic differential equations. In: ICLR (2022)
49. Mirza, M., Osindero, S.: Conditional generative adversarial nets. CoRR **abs/1411.1784** (2014)
50. Mittal, G., Engel, J.H., Hawthorne, C., Simon, I.: Symbolic music generation with diffusion models. In: ISMIR (2021)
51. Miyoshi, M., Kaneda, Y.: Inverse filtering of room acoustics. IEEE Trans. Audio Speech Lang. Process. **36**(2), 145–152 (1988)
52. Murgai, P., Rau, M., Jot, J.M.: Blind estimation of the reverberation fingerprint of unknown acoustic environments. In: Audio Engineering Society Convention 143. Audio Engineering Society (2017)
53. Nakatani, T., Bölddeker, C., Kinoshita, K., Ikeshita, R., Delcroix, M., Haeb-Umbach, R.: Jointly optimal denoising, dereverberation, and source separation. IEEE Trans. Audio Speech Lang. Process. **28**, 2267–2282 (2020)
54. Nakatani, T., Yoshioka, T., Kinoshita, K., Miyoshi, M., Juang, B.H.: Speech dereverberation based on variance-normalized delayed linear prediction. IEEE Trans. Audio Speech Lang. Process. **18**(7), 1717–1731 (2010)
55. Naylor, P.A., Gaubitch, N.D., et al.: Speech dereverberation, vol. 2. Springer (2010)
56. Nichol, A.Q., Dhariwal, P.: Improved denoising diffusion probabilistic models. In: ICML (2021)
57. Nichol, A.Q., Dhariwal, P., Ramesh, A., Shyam, P., Mishkin, P., McGrew, B., Sutskever, I., Chen, M.: GLIDE: towards photorealistic image generation and editing with text-guided diffusion models. In: ICML (2022)
58. Panayotov, V., Chen, G., Povey, D., Khudanpur, S.: Librispeech: An ASR corpus based on public domain audio books. In: ICASSP (2015)
59. Radford, A., Kim, J.W., Hallacy, C., Ramesh, A., Goh, G., Agarwal, S., Sastry, G., Askell, A., Mishkin, P., Clark, J., Krueger, G., Sutskever, I.: Learning transferable visual models from natural language supervision. In: ICML (2021)
60. Radford, A., Metz, L., Chintala, S.: Unsupervised representation learning with deep convolutional generative adversarial networks. In: ICLR (2016)
61. Rennies, J., Brand, T., Kollmeier, B.: Prediction of the influence of reverberation on binaural speech intelligibility in noise and in quiet. The Journal of the Acoustical Society of America **130**(5), 2999–3012 (2011)
62. Rix, A.W., Beerends, J.G., Hollier, M.P., Hekstra, A.P.: Perceptual evaluation of speech quality (pesq)-a new method for speech quality assessment of telephone networks and codecs. In: ICASSP (2001)
63. Saharia, C., Chan, W., Saxena, S., Li, L., Whang, J., Denton, E.L., Ghasemipour, S.K.S., Lopes, R.G., Ayan, B.K., Salimans, T., Ho, J., Fleet, D.J., Norouzi, M.: Photorealistic text-to-image diffusion models with deep language understanding. In: NeurIPS (2022)

64. Savioja, L., Xiang, N.: Simulation-based auralization of room acoustics. *Acoust. Today* **16**(4), 48–55 (2020)
65. Schroeder, M.R., Logan, B.F.: "colorless" artificial reverberation. *IRE Transactions on Audio* (6), 209–214 (1961)
66. Shah, M., Chen, X., Rohrbach, M., Parikh, D.: Cycle-consistency for robust visual question answering. In: *CVPR* (2019)
67. Singh, A., Hu, R., Goswami, V., Couairon, G., Galuba, W., Rohrbach, M., Kiela, D.: FLAVA: A foundational language and vision alignment model. In: *CVPR* (2022)
68. Singh, N., Mentch, J., Ng, J., Beveridge, M., Drori, I.: Image2reverb: Cross-modal reverb impulse response synthesis. In: *ICCV* (2021)
69. Sohl-Dickstein, J., Weiss, E.A., Maheswaranathan, N., Ganguli, S.: Deep unsupervised learning using nonequilibrium thermodynamics. In: *ICML* (2015)
70. Song, J., Meng, C., Ermon, S.: Denoising diffusion implicit models. In: *ICLR* (2021)
71. Su, J., Jin, Z., Finkelstein, A.: Acoustic matching by embedding impulse responses. In: *ICASSP* (2020)
72. Sunkara, R., Luo, T.: No more strided convolutions or pooling: A new CNN building block for low-resolution images and small objects. In: *ECML* (2022)
73. Tan, H., Yu, L., Bansal, M.: Learning to navigate unseen environments: Back translation with environmental dropout. In: *NAACL* (2019)
74. Tan, K., Xu, Y., Zhang, S., Yu, M., Yu, D.: Audio-visual speech separation and dereverberation with a two-stage multimodal network. *IEEE J. Sel. Top. Signal Process.* **14**(3), 542–553 (2020)
75. Välimäki, V., Parker, J.D., Savioja, L., III, J.O.S., Abel, J.S.: Fifty years of artificial reverberation. *IEEE Trans. Speech Audio Process.* **20**(5), 1421–1448 (2012)
76. Vaswani, A., Shazeer, N., Parmar, N., Uszkoreit, J., Jones, L., Gomez, A.N., Kaiser, L., Polosukhin, I.: Attention is all you need. In: *NeurIPS* (2017)
77. Wang, H., Liang, W., Shen, J., Gool, L.V., Wang, W.: Counterfactual cycle-consistent learning for instruction following and generation in vision-language navigation. In: *CVPR* (2022)
78. Wang, P., Yang, A., Men, R., Lin, J., Bai, S., Li, Z., Ma, J., Zhou, C., Zhou, J., Yang, H.: OFA: unifying architectures, tasks, and modalities through a simple sequence-to-sequence learning framework. In: *ICML* (2022)
79. Wang, Y., Wang, W., Liang, W., Yu, L.: Comic-guided speech synthesis. *ACM Trans. Graph.* **38**(6), 187:1–187:14 (2019)
80. Wu, B., Li, K., Ge, F., Huang, Z., Yang, M., Siniscalchi, S.M., Lee, C.H.: An end-to-end deep learning approach to simultaneous speech dereverberation and acoustic modeling for robust speech recognition. *IEEE Journal of Selected Topics in Signal Processing* **11**(8), 1289–1300 (2017)
81. Wu, B., Li, K., Yang, M., Lee, C.: A reverberation-time-aware approach to speech dereverberation based on deep neural networks. *IEEE Trans. Audio Speech Lang. Process.* **25**(1), 98–107 (2017)
82. Xie, Q., Dai, Z., Hovy, E.H., Luong, T., Le, Q.: Unsupervised data augmentation for consistency training. In: *NeurIPS* (2020)
83. Yang, Z., Chen, G., Li, X., Wang, W., Yang, Y.: Doraamongpt: Toward understanding dynamic scenes with large language models. In: *ICML* (2024)
84. Yi, Z., Zhang, H.R., Tan, P., Gong, M.: Dualgan: Unsupervised dual learning for image-to-image translation. In: *ICCV* (2017)
85. Zhang, Y., Xiang, T., Hospedales, T.M., Lu, H.: Deep mutual learning. In: *CVPR* (2018)

86. Zhao, Y., Wang, D., Xu, B., Zhang, T.: Monaural speech dereverberation using temporal convolutional networks with self attention. *IEEE Trans. Audio Speech Lang. Process.* **28**, 1598–1607 (2020)
87. Zhao, Y., Wang, Z., Wang, D.: Two-stage deep learning for noisy-reverberant speech enhancement. *IEEE Trans. Audio Speech Lang. Process.* **27**(1), 53–62 (2019)
88. Zhao, Z., Xia, Y., Qin, T., Xia, L., Liu, T.: Dual learning: Theoretical study and an algorithmic extension. In: *ACML* (2020)

## Supplementary Materials

In the appendix, we provide the following content for a more comprehensive understanding of our method:

- § A: **Architecture Details**. We provide details of the MVSD network architecture, including layer composition, connectivity patterns, *etc.*
- § B: **Social Impacts and Limitations**.
- § C: **Qualitative Visualization** of MVSD and several competitors.

### A Architecture Details

Our neural network draws inspiration from the Unet structure of Imagen [63]. Taking VAM as an example, in each step of diffusion, the controllable Unet learns to perform cross-modal generation using noisy input, clean spectrograms, and embeddings of the visual environment. As shown in Fig. A1, we divide controllable Unet into encoder and decoder with symmetric structure and both of them consist of 3 attention blocks. Skip connections [24] are employed to bridge encoder and decoder, recovering spatial information lost in downsampling. We only apply cross-modal attention [76] in the third block of the encoder and the first block of the decoder to connect visual cues and spectrograms. In self-attention block, we utilize the downsampling module [72] with a stride of 4 to rapidly reduce the size of the feature map. The feature map undergoes a size transformation in the controllable Unet ( $128^2 \rightarrow 32^2 \rightarrow 8^2 \rightarrow 4^2 \rightarrow 8^2 \rightarrow 32^2 \rightarrow 128^2$ ). The diffusion training process involves the following steps: starting with a sample from the data distribution, noise is gradually added over a fixed number of timesteps, creating a sequence of increasingly noisy images to reconstruct the original input. During inference, the goal is to generate samples from the learned distribution by starting with pure noise and sequentially applying the trained UNet model to denoise the image over timesteps.

### B Social Impacts and Limitations

MVSD can enrich VR and AR auditory experiences with more realistic acoustics that complement the protagonist’s surroundings. VAM can enhance personalized advertis-

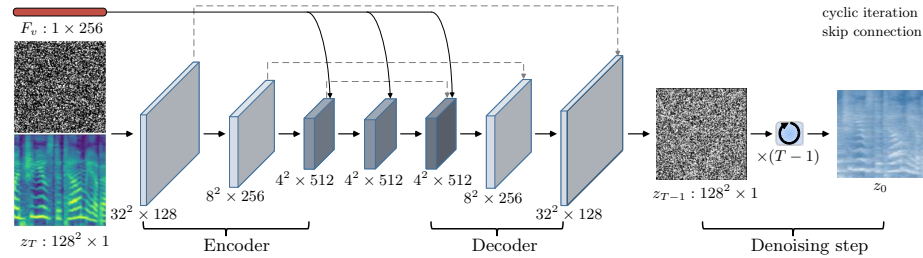


**Fig. A1:** Overview of the controllable Unet: MVSD utilizes a frozen visual scene encoder to encode an input RGB image into a visual feature  $F_v$  which is then mapped to a  $128 \times 128$  spectrogram by Controllable Unet, facilitating auditory style transformations (§A).

ing, assistive technologies, and speech synthesis and recognition. Furthermore, dereverberation task can boost speech audibility across various environments, reducing reverberation for clearer communication in teleconferencing, broadcasting, and public spaces. Nevertheless, there are potential risks concerning privacy, possible misuse, and ethics, notably in diverse societal backgrounds.

While MVSD presents a promising potential, there is still scope for further exploration and investigation. Diffusion models require more time for training and sampling than GANs, posing significant challenges for real-time applications such as meetings and sound rendering, *etc.* Future efforts will focus on how to integrate methods like [70] and [44] to reduce the number of parameters and speed up diffusion models.

## C Qualitative Visualization

This section showcases visualizations of qualitative results for our MVSD and competing methods. Among them, Fig. A2 and Fig. A3 depict the qualitative results of the VAM task on different datasets. Fig. A4 showcases the visualization of the generated results on SoundSpaces-Speech dataset in the dereverberation task. Fig. A5 illustrates some instances of failure cases observed on SoundSpaces-Speech dataset [4].

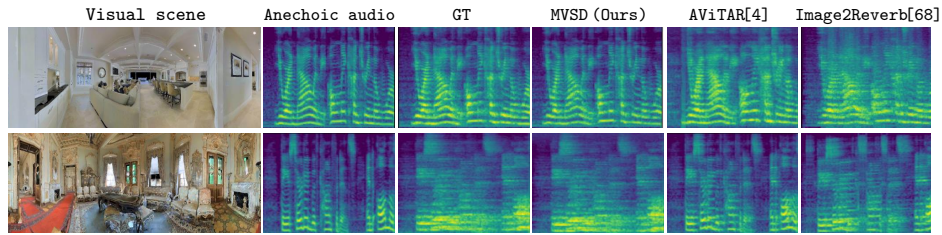


**Fig. A2:** Visualization results on SoundSpaces-Speech dataset in VAM task (§C).

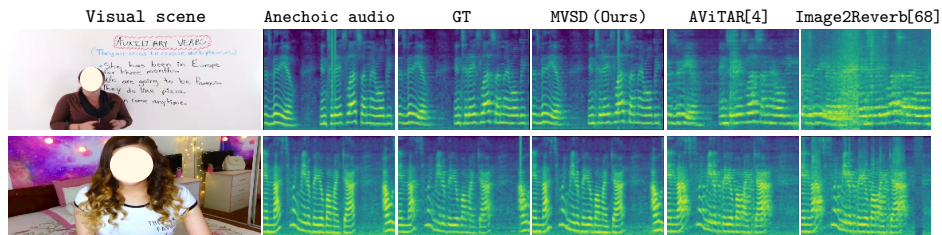


**Fig. A3:** Visualization results on AVSpeech dataset in VAM task (§C).

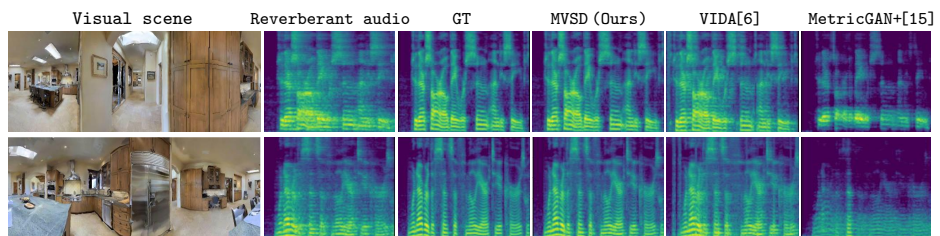


Fig. A4: Visualization on SoundSpaces-Speech dataset in dereverberation task (§C).

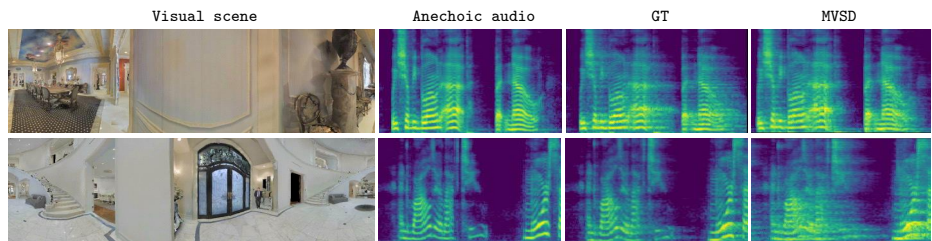


Fig. A5: Some failed samples from SoundSpaces-Speech dataset in VAM task (§C).